STARS

1-1-2006

Phase-and-amplitude regeneration of differential phase-shift keyed signals using a phase-sensitive amplifier

Kevin Croussore
University of Central Florida

Inwoong Kim
University of Central Florida

Cheolhwan Kim
University of Central Florida

Yan Han
University of Central Florida

Guifang Li
University of Central Florida
Find similar works at: https://stars.library.ucf.edu/facultybib2000

University of Central Florida Libraries http://library.ucf.edu

Recommended Citation

Croussore, Kevin; Kim, Inwoong; Kim, Cheolhwan; Han, Yan; and Li, Guifang, "Phase-and-amplitude regeneration of differential phase-shift keyed signals using a phase-sensitive amplifier" (2006). *Faculty Bibliography 2000s*. 4676.
https://stars.library.ucf.edu/facultybib2000/4676

Phase-and-amplitude regeneration of differential phase-shift keyed signals using a phase-sensitive amplifier

Kevin Croussore, Inwoong Kim, Cheolhwan Kim, Yan Han and Guifang Li

CREOL and FPCE, The College of Optics and Photonics, University of Central Florida, 4000 Central Florida boulevard, Orlando, FL, 32816
kcrousso@creol.ucf.edu ,li@creol.ucf.edu

Abstract – DPSK phase-and-amplitude regeneration with a NOLM-based phase-sensitive amplifier is demonstrated experimentally. For a highly degraded input signal, maximum differential phase errors were reduced from 82° to 41°, while the SNR was improved by more than 5-dB. Differential phase Q-factor improvement was better than 6-dB. The PSA was operated free of excess noise due to stimulated Brillouin scattering by using a binary phase modulated pulse train as the pump. The impact of pump fluctuations on regeneration performance is clarified. The regenerated signal was characterized by measurement of the constellation diagram by linear optical sampling, giving the first directly measured evidence of DPSK phase regeneration.

© 2006 Optical Society of America

OCIS codes: (060.4370) Nonlinear optics, fibers; (060.4510) Optical communications; (060.5060) Phase modulation; (060.2330) Fiber optics communication; (190.4380) Nonlinear optics, four-wave mixing

---

References

1. C. Xu, X. Liu and X. Wei, "Differential phase-shift keying for high spectral efficiency optical transmissions," IEEE J. Sel. Top. Quantum Electron. **10**, 281-293 (2004).
2. C. J. McKinstrie, C. Xie and C. Xu, "Efects of cross-phase modulation on phase jitter in soliton systems with constant dispersion," Opt. Lett. **28**, 604-606 (2003).
3. A. Striegler and B. Schmauss, "All-optical DPSK signal regeneration based on cross-phase modulation," IEEE Photonics Technol. Lett. **16**, 1083-1085 (2004)
4. A. Striegler, M. Meissner, K. Cvecek, K. Sponsel, G. Leuchs and B. Schmauss, "NOLM-based RZ-DPSK signal regeneration," IEEE Photon. Technol. Lett. **17**, 639-641 (2005).
5. M. Matsumoto, "Regeneration of RZ-DPSK signals by Fiber-based all-optical regenerators," IEEE Photonics Technol. Lett. **17**, 1055-1057 (2005).
6. C. Pare, A. Villeneuve, P. A. Belanger and N. J. Doran, "Compensating for dispersion and the nonlinear Kerr effect without phase conjugation," Opt. Lett. **21**, 459-461 (1996).
7. I. R. Gabitov and P. M. Lushnikov, "Nonlinearity management in a dispersion managed system," Opt. Lett. **27**, 113-115 (2002).
8. S. L. Jansen, D. van den Borne, G. D. Khoe, H. de Waardt, C. C. Monsalve, S. Spalter and P. M. Krummrich, "Reduction of nonlinear phase noise by mid-link spectral inversion in a DPSK based transmission system," in Proceedings of the Conference on Optical Fiber Communications (OFC) (Optical Society of America, 2005) OTh05.
9. X. Liu, X. Wei, R. E. Slusher and C. J. McKinstrie, "Improving transmission performance in differential phase-shift-keyed systems by use of lumped nonlinear phase-shift compensation," Opt. Lett. **27**, 1616-1618 (2002).
10. C. Xu and X. Liu, "Post-nonlinearity compensation with data-driven phase modulators in phase-shift keying transmission," Opt. Lett. **27**, 1619-1621 (2002).
11. M. Shin, P. S. Devgan, V. S. Grigoryan and P. Kumar, "SNR Improvement of DPSK signals in a semiconductor optical regenerative amplifier," IEEE Photonics Technol. Lett. **18**, 49-51 (2006).
12. M. E. Marhic, C. H. Hsia and J. M. Jeong, "Optical Amplification in a nonlinear fiber interferometer," Electron. Lett. **27**, 210-211 (1991).

13. W. Imajuku, A. Takada and Y. Yamabayashi, "Inline coherent optical amplifier with noise figure lower than 3 dB quantum limit," Electron. Lett. **36**, 63-64 (2000).
14. G. D. Bartolini, D. K. Serkland, P. Kumar and W. L. Kath, "All-optical storage of a picosecond-pulse packet using parametric amplification," IEEE Photonics. Technol. Lett. **9**, 1020-1022 (1997).
15. A. Takada and W. Imajuku, "Amplitude noise suppression using a high gain phase sensitive amplifier as a limiting amplifier," Electron. Lett. **32**, 677-679 (1996).
16. H. P. Yuen, "Reduction of quantum fluctuation and suppression of the Gordon-Haus effect with phase-sensitive linear amplifiers," Opt. Lett. **17**, 73-75 (1992).
17. K. Croussore, C. Kim and G. Li, "All-optical regeneration of differential phase-shift keying signals based on phase-sensitive amplification," Opt. Lett. **29**, 2357-2359 (2004).
18. K. Croussore, I. Kim, Y. Han, C. Kim and G. Li, "Demonstration of phase-regeneration of DPSK signals based on phase-sensitive amplification," Opt. Express **13**, 3945-3950 (2005).
19. K. Croussore, C. Kim and G. Li, "All-optical regeneration of differential phase-shift keyed signals based on phase-sensitive amplification," in Proc. SPIE Defense and Security Symposium, **5814**, 166-175 (2005).
20. C. J. McKinstrie and S. Radic, "Phase-sensitive amplification in a fiber," Opt. Express **20**, 4973-4979 (2004).
21. C. Dorrer, C. R. Doerr, I. Kang, R. Ryf, J. Leuthld and P. J. Winzer, "Measurement of eye diagrams and constellation diagrams of optical sources using linear optics and waveguide technology," J. Lightwave Technol. **23**, 178-186 (2005).
22. C. Dorrer, "Complete characterization of periodic optical sources by use of sampled test-plus-reference interferometry," Opt. Lett. **30**, 2022-2024 (2005).
23. I. Kim, C. Kim and G. Li, "Requirements for the sampling source in coherent linear sampling," Opt. Express **12**, 2723-2730 (2004).
24. R. Li, P. Kumar and W. L. Kath, "Dispersion compensation with phase-sensitive optical amplifiers," J. Lightwave Technol. 12, 541-549 (1994).
25. Norimatsu, S.; Iwashita, K.; Noguchi, K, "An 8 Gb/s QPSK optical homodyne detection experiment using external-cavity laser diodes," IEEE Photonics Technol. Lett. **4** (7), 765-767 (1992).
26. K. Croussore, C. Kim, R. Schiek and G. Li, "All-optical regeneration of DPSK signals based on phase-sensitive amplification," presented at Optics in the Southeast, OSA Regional Meeting, Charlotte NC (November 4-6, 2004).

1. Introduction

Differential phase-shift keying (DPSK) has emerged as the leading modulation format for long-haul communications systems. At high bit rates and small channel spacing required for dense wavelength-division multiplexing (DWDM), DPSK offers advantages over on-off keying (OOK) including a 3-dB improvement in receiver sensitivity and enhanced tolerance to fiber nonlinearities. Because the information is encoded in differential phase shifts between pulses, DPSK systems are much more sensitive to phase noise (PN) than amplitude noise (AN). In fact the accumulation of linear and nonlinear phase noise limits transmission distance when timing jitter is not a factor [1]. As a result the bit-error-ratio (BER) performance of DPSK systems is predominantly determined by the phase noise statistics rather than amplitude noise statistics. Linear phase noise is introduced by phase modulators and phase-insensitive amplifiers (PIAs) such as erbium-doped fiber amplifiers through amplified spontaneous emission (ASE). Nonlinear phase noise arises when AN converts to PN through fiber nonlinearity, commonly known as the Gordon-Mollenauer effect. In such nonlinear transmission systems the growth of the phase noise variance with transmission length is expected to be cubic [2]. In order to maximize the reach of future DPSK systems it is required to manage the accumulation of both amplitude noise and phase noise. Several methods have been analyzed for providing amplitude regeneration of DPSK signals [3-5], however to our knowledge these have not been demonstrated experimentally. Nonlinearity management [6, 7], spectral inversion [8] and post-transmission nonlinear phase shift compensation (NLPSC) [9, 10] have been proposed as methods for reducing the accumulation of PN or compensating PN after transmission. Typically, these schemes are complex to implement and the NLPSC scheme is effective mainly for mitigating effects of self-phase modulation (SPM). Some small SNR improvements in DPSK have been achieved using a semiconductor device similar to a NOLM [11].

Recently fiber-based phase-sensitive amplifiers (PSAs) have been analyzed [12] and demonstrated [13] for amplification of signals without the addition of spontaneous emission noise, resulting in a noise figure less than the 3-dB quantum limit of a PIA. . PSAs also exhibit regenerative characteristics when used to store soliton pulses in optical buffers [14] and may act as high-speed limiting amplifiers for OOK signals [15]. While all modulation formats will benefit from the low noise amplification properties of PSAs, DPSK in particular benefits from using a PSA rather than a PIA. It has been suggested [16] and shown both analytically [17] and experimentally [18] that, in addition to amplifying without the addition of ASE noise, a PSA has phase-regenerative properties for DPSK signals. In Refs. [17, 19] we proposed combining the phase-regenerative and limiting amplification properties of the PSA to regenerate DPSK signals. Simulations show that for an optimized PSA, remarkably good phase regeneration is still obtained for signals suffering large amplitude noise. While several methods have been analyzed for producing fiber-compatible PSAs [20], the NOLM-based PSA offers a simple solution for combining phase-and-amplitude regeneration in a single device. In this paper the first experimental demonstration of DPSK phase-and-amplitude regeneration using a NOLM-based phase sensitive amplifier is presented.

2. Experimental setup

The setup for the DPSK regeneration experiment is shown in Fig. 1. 10 Gb/s RZ-DPSK data with 33% duty cycle and pattern length of at least 2^{11}-1 was generated using a phase modulator and Mach-Zehnder intensity modulator. The data was amplified by an EDFA and separated into a pump (for the PSA) and signal (to be regenerated) using a 90/10 splitter. As previously described, the use of a binary phase modulated pump eliminates excess noise due to Stimulated Brillouin Scattering [18, 19]. Different path lengths for the pump and signal ensure de-correlation of the PRBS data by > 50 bits. Phase and amplitude noise were added to the signal using two additional modulators, which were driven sinusoidally. This allowed independent adjustment of the relative AN and PN levels. For example, the differential PN variance could be increased without changing AN to simulate a signal that suffers nonlinear phase noise, rather than ASE-type linear phase noise. The noise frequencies were typically different, with $f_{AN} > 6$ GHz and f_{PN} determined by mixing the synthesizer output with the 10 GHz clock signal from the BERT: $f_{PN} = 10 GHz - f_{AN} \leq 4 GHz$. For constellation diagram measurements (Section 4.3) the noise frequencies were synchronized to integer multiples of the sampling frequency of the oscilloscope, which is 6.25 GHz. In both cases the DPSK signal acquires a pseudo-random noise pattern such that bits of all amplitudes acquire phase errors ranging from zero to the maximum over a period of a few tens of bits. This is important since the operation of the PSA as a DPSK regenerator is highly sensitive to the particular combination of amplitude and phase of each bit. The addition of PN is quantified in terms of the maximum phase error, where $MPE = \max(\phi_{n-1} - \phi_n)$ is the maximum deviation of all detected differential phases from original encoded values. Note that logical errors are only produced for $MPE > 90°$. An optical attenuator is used to adjust the pump to signal power ratio from 10 to ~20 dB at the input, limited by the available pumping power. A free-space delay line in the pump path allows temporal alignment of the pump and signal pulses at the PSA input as well as a method for manually scanning the input phase difference. Input phase drift was stabilized by a phase-lock loop that monitors the signal gain and drives a fiber stretcher. The PSA was comprised of a 3-dB coupler and 6058 meters of HNLF (not polarization maintaining) with a total insertion loss of 5 dB and effective nonlinear coefficient of 9.75 W^{-1}km^{-1}. An intra-loop polarization controller was required to maximize reflection of the pump and transmission of the regenerated signal, which was extracted by the optical circulator, tapped for feedback, and sent to a DPSK demodulator and BER tester or oscilloscope for detection.
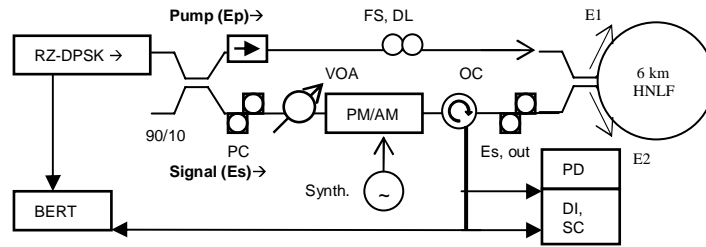
Fig. 1. Experimental setup. FS, DL: fiber stretcher, delay line; VOA: optical attenuator; OC: optical circulator; PC: polarization controller; PD: photodiode; DI, SC: delay interferometer + sampling oscilloscope; Synth: synthesizer; BERT: bit-error-ratio tester; PM/AM: noise adding phase and amplitude modulators.

3. Configuration of PSA for phase-and-amplitude regeneration

In Refs. [17, 19] the operation of the PSA as a DPSK regenerator was described in detail. The pump and signal combine to form two counter-propagating waves E1 and E2. If the pump and signal are in-phase at the input the optical powers P1 and P2 are the same and the interferometer is balanced: pump light is reflected to the pump input port and signal light through the signal input port. For non-zero input phase difference P1 and P2 differ, and the fields accumulate different nonlinear phase shifts due to SPM. This allows pump light to be transferred to the signal output port at recombination resulting in signal amplification. The signal gain is determined by the quantity $\gamma \cdot L_{eff} \cdot \sqrt{Pp(0) \cdot Ps(0)} \cdot \sin(\delta) \equiv \left|\varphi_{ps}\right| \cdot \sin(\delta)$, where δ is

the pump to signal phase difference at the input, *Pp(0)* and *Ps(0)* are the pump and signal input powers and γ is the fiber nonlinear coefficient. This quantity is the accumulated phase-difference between E1 and E2 inside the interferometer. For the NOLM-PSA, $\delta = \pi/2$ is required to maximize φ_{ps} (referred to as the nonlinear phase shift, or NLPS). Phase regeneration is achieved since the signal quadrature component is strongly amplified while components nearly in-phase are attenuated [19]. Phase regeneration may be accomplished with values of φ_{ps} of the order of 0.2π, regardless of the input AN level. Combining phase and amplitude regeneration requires $\varphi_{ps} \sim 0.5\pi$. Simulations indicate that the exact value that maximizes the output SNR depends strongly on the amount of input PN. However the SNR is still improved for a relatively large range of NLPS around 0.5π. Experimentally the value of NLPS can be estimated by observing the characteristics of the phase-sensitive gain. Figure 2 shows the measured (a-d) and calculated (e-h) signal power (versus input phase δ) for different values of NLPS. For experiments, the input phase difference is deterministically varied by rotating the free space delay line. The amplified signal is then recorded as a function of time on an optical spectrum analyzer operating in zero-span mode. The time axis may be correlated to relative phase for each case, although the phase-scanning rate varies slightly between cases. The dashed line represents the background signal power (in absence of pump) while solid lines show the amplified signal with pump leakage subtracted. Some small fluctuations in the background signal power result from environmental fluctuations and interferometric instabilities. Calculations in Fig. 2(e-h) are based on the depleted-pump analysis [e.g., 12, 19], neglecting dispersion of the relatively short fiber. At small NLPS the gain profile was nearly sinusoidal as in previous reports. Note that when NLPS < 0.5π the value of δ that leads to maximum gain differs from 0.5π by a deterministic amount, and that when $\delta = \pi$, 2π the gain is unity [19]. As NLPS increases beyond 0.5π the profile develops additional oscillations, and the quadrature gain is reduced. The condition of NLPS = 0.5π is held for all regeneration experiments by obtaining a flattened gain peak as shown in Figs. 2

(c) and (g). Simultaneous regeneration is optimized by varying the input pump-to-signal power ratio $\Gamma = P_p(0)/P_s(0)$, which also determines the maximum signal gain. In the theory, increasing Γ (for NLPS = 0.5π) decreases the ratio of in-phase to quadrature gain, which sets the limit for the smallest ratio of output to input phase fluctuations [19]. Similarly, when the input signal PN large, output amplitude fluctuations are reduced by increasing Γ.
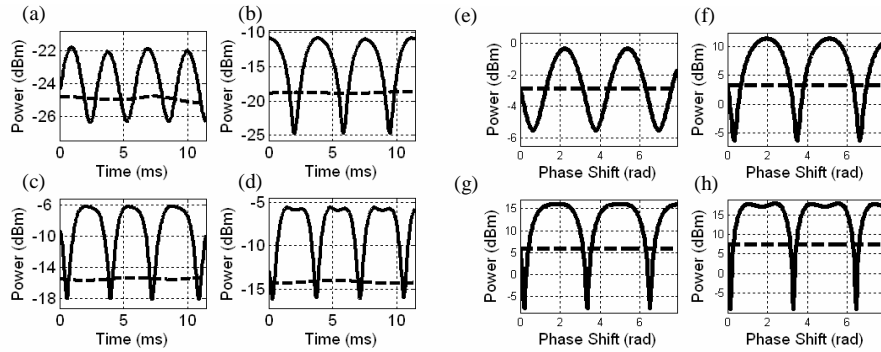

Fig. 2. Measured (a-d) and calculated (e-h) signal output power versus relative input phase for the PSA for NLPS of 0.1π, 0.25π, 0.5π and 0.55π. Solid lines: amplified signal, dotted lines: transmitted signal power in the absence of the pump.

4. Results of phase-and-amplitude regeneration

4.1.   Amplitude regeneration

The addition of amplitude noise, as well as amplitude regeneration, was monitored by observing the intensity waveform and eye diagram since as shown below the demodulated eye is not sensitive to high frequency AN. Figure 3(a) shows the back-to-back intensity eye when AN was added at a random frequency near 6 GHz. The electrical SNR, defined as average of all peak powers divided by the standard deviation of this distribution, is degraded to approximately 5.8 dB at a received power of 1 dBm. The degraded signal waveform is visualized in Fig. 3(c) by adding similar AN at the sampling frequency of the scope (6.25 GHz). Large bit-to-bit amplitude shifts are generated similar to those acquired by a realistic DPSK signal after transmission. The corresponding PN source adds maximum phase errors slightly greater than 80°, and in all results reported herein the input suffers from both PN and AN. The PSA was operated with an average pump power of 93 mW (peak power just over 200 mW) and a pump to signal power ratio of almost 12 dB. Without the pump present the transmitted signal power was 300 μW, and the pump leakage detected through the signal port was around 30 μW. The amplified signal power was 4.25 mW corresponding to 11.5 dB of gain, although under stable phase-locking the output power was reduced somewhat to 3.95 mW (11.2 dB gain). The net gain and observed phase-sensitive gain profile (Fig. 2) agree with generation of NLPS = 0.5π.

Figure 3(b) shows a typical intensity eye diagram of the phase-and-amplitude regenerated DPSK signal, at the same received power of 1 dBm as in Fig. 3(a). The improvement in AN statistics is clearly evident. The output SNR reaches nearly 11 dB, corresponding to 5 dB of improvement. Figure 3(d) shows considerably smaller amplitude fluctuations for the regenerated signal, proving the amplitude regeneration property of the PSA to be robust with respect to the presence of phase noise. A short sample of the waveform is shown for clarity, however similar results are obtained regardless of which time interval is chosen. This is reflected in the SNR improvement of 5 dB, which accounts for many repetitions of the entire PRBS pattern.
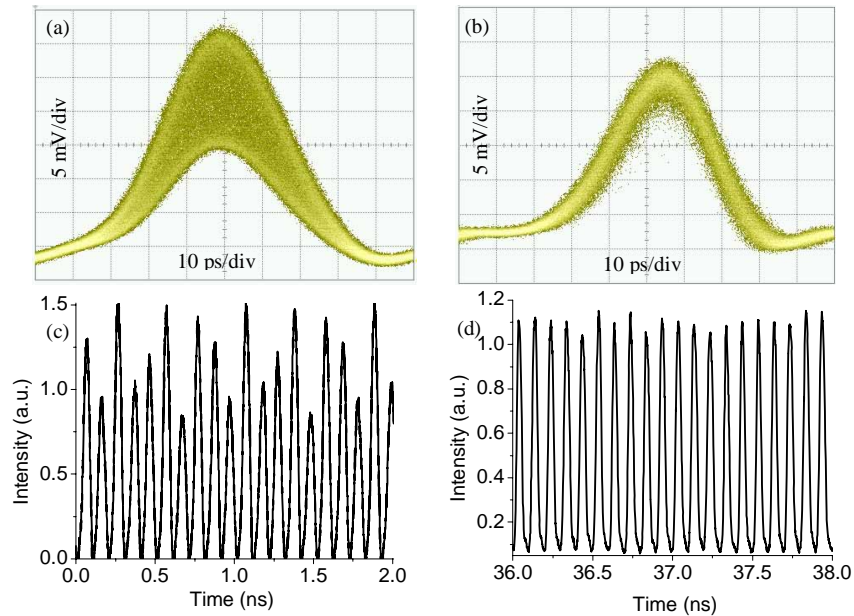
Fig. 3. Signal waveform (a) back to back with added PN and AN and (b) after regeneration. AN is added at the sampling frequency of the oscilloscope (6.25 GHz). Intensity eye diagram (c) back to back with SNR of 5.75 dB, and (d) after regeneration for the same received power with an improved SNR of 11 dB.

4.2. Phase regeneration and BER

In Fig. 4 the demodulated eye diagram of the DPSK signal is visualized before and after combined phase-and-amplitude regeneration. The back-to-back eye is shown without any added noise in 4(a), with added AN in 4(b) and with both PN and AN added in 4(c). The addition of PN in Fig. 4(c) at a frequency near 4 GHz leads to a severely reduced eye opening. The fact that the eye is nearly closed proves the added PN produces differential phase errors approaching 90° (the threshold for producing a logical error). After regeneration the eye, shown on the same scale and for the same received power in Fig. 4(d), was clearly open indicating highly effective removal of phase noise. From the obvious improvement in demodulated eye Q-factor one expects a strong improvement in the differential phase statistics, with a related improvement in BER performance. The slight residual eye closure indicates the presence of phase noise after regeneration, resulting primarily from signal AN to PN conversion. Some small, additional fluctuations in both amplitude and phase result from the transfer of pump fluctuations.

BER performance was measured for back-to-back degraded signals with AN only and with PN and AN, and after regeneration for the cases described above. The received power is measured at the input to the delayed interferometer, without pre-amplification by an additional EDFA. Thus the results in Fig. 5 are useful for comparing BER performance of the signals but do not suggest the actual receiver sensitivity that would be obtained. The results shown in Fig. 5 demonstrate the effectiveness of the DPSK regeneration process. Without regeneration, the back-to-back signal reaches an error floor approaching 10^{-9} at a received power of 0 dBm when both PN and AN are added, indicating the presence of logical errors. The regenerated signal must exhibit the same error floor since the PSA (or any other regeneration scheme) may not remove phase errors that have already accumulated. However a negative power penalty of nearly 6 dB is clearly demonstrated, and for the same received power the BER was reduced by up to 7 orders of magnitude. This indicates the removal of

signal phase noise despite the presence of large amplitude noise at the input. For reference the BER of the back-to-back signal with only added AN is shown as well, indicating that even though the SNR was highly degraded by adding AN, the BER performance is not strongly affected.
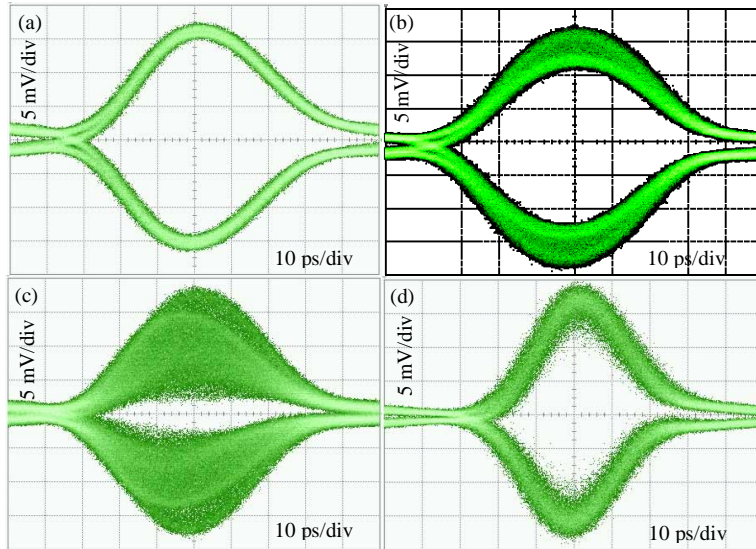

Fig. 4. Demodulated eye diagrams. Back to back with (a) no added noise; (b) with added AN only and (c) with PN and AN added. Note the lack of eye closure for the AN-only case. (d) Demodulated eye after phase-amplitude regeneration.
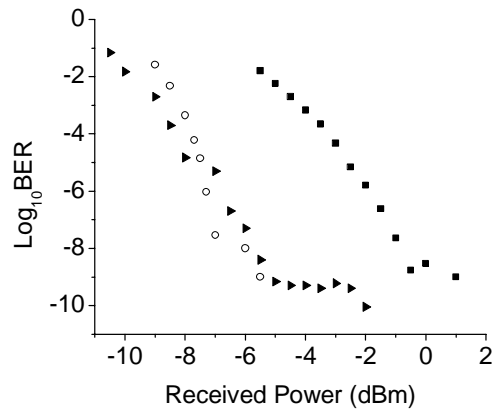

Fig. 5. BER curves for back-to-back degraded data (squares) and regenerated data (triangles). Negative power penalty is 5 dB. Empty circles represent back-to-back data with only amplitude noise added.

4.3. Measurement of the constellation diagram

Although the intensity eye and waveform may fully characterize the amplitude statistics of DPSK signals, observation of the demodulated eye diagram does not fully disclose all the information about the signal phase properties. To fully characterize the signal it is useful to plot the constellation diagram, which is typically done in simulations of DPSK transmission and regeneration. From this diagram the differential phase statistics are calculated in a straightforward manner. Experimentally, the technique of linear optical sampling can be used

to measure signal amplitude and phase [21-23]. Normally the technique when applied to high speed signals requires a sophisticated pulsed local oscillator. However in the present case, a simple CW local oscillator derived from the same source as the pump and signal has been used. This is sufficient for measuring highly periodic signals, requiring only that PN and AN be added at multiples of the same frequency. In Fig. 6 the directly measured constellation diagram, amplitude histogram and calculated differential phase (with distribution superimposed) are shown for three cases. All data were obtained by sampling periodically at the bit rate, so each data point represents the peak amplitude and phase of a single bit near the bit center.
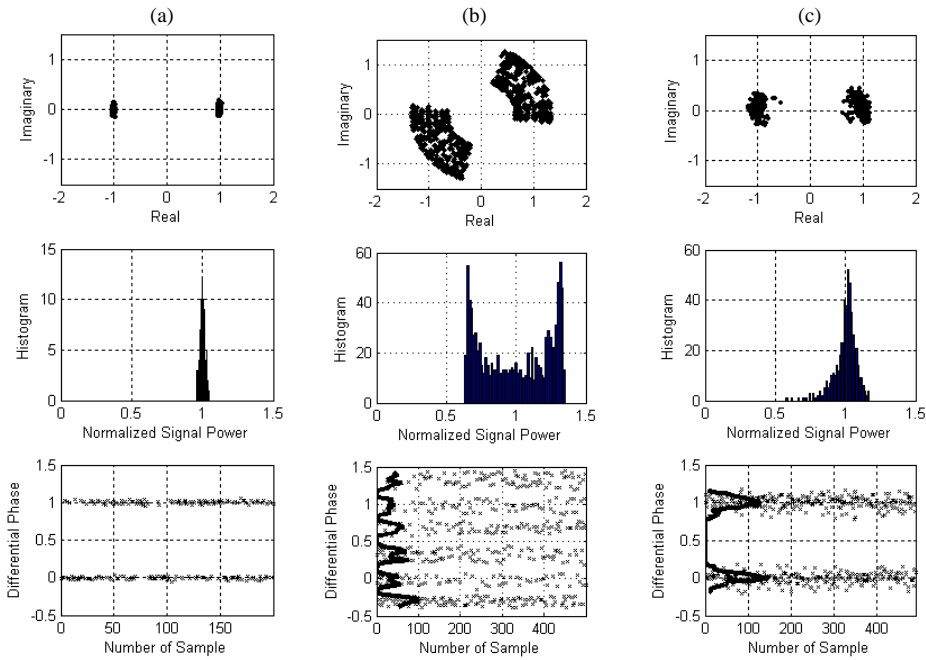

Fig. 6. From top to bottom: directly measured constellation diagram, histogram of signal power sampled at bit center and calculated differential phase (crosses) with distribution super-imposed (solid line). Back to back signal (a) with no added noise and (b) with added PN and AN. (c) Signal after phase-and-amplitude regeneration.

The back-to-back signal was first measured without the addition of any additional noise. Since phase modulation is applied (the DPSK data) this does not give a limit of the measurement accuracy, but reveals the phase noise present on both the pump and signal. The origin of the phase noise is the electrical signal driving the modulator, which exhibits pattern effects as well as asymmetric and relatively slow rise and fall times. The data of Fig. 6(a) indicate the angular width of the encoded $0, \pi$ phase states each to be around 10°. Differential phase noise of the same order is present and visible in the graph at the bottom of Fig. 6(a). This phase noise contribution was quite small compared to the PN added to the signal intentionally. It is the fact that it exists on the pump wave as well that has repercussions for the operation of the PSA. Residual amplitude noise shown in the histogram reflects small signal intensity pattern effects generated by the pulse carver. Without noise addition, the SNR was 17.6 dB and the calculated differential phase Q-factor was 14.3 dB.

Figure 6(b) shows the back-to-back signal with phase and amplitude noise added for a series of 400 consecutive bits. The constellation diagram shows nearly uniformly distributed noise for the case of AN added at 6.25 GHz and PN added at 3.125 GHz, representing all

relevant combinations of input amplitude and phase. The degraded SNR was 5.75 dB, and calculated differential phase Q-factor was only 2.64 dB. The maximum measured differential phase error from the lower plot was 82°. The data after regeneration are shown in Fig. 6(c). The improvement in the signal constellation diagram (top) is clear: both PN and AN were significantly reduced. The SNR and differential phase-Q were both improved by 6 dB, to 11 dB and 8.2 dB respectively, and the maximum phase error was reduced from 82° to 41°. This is by far the largest reduction in signal phase noise presented to date, by any means. It was observed that much better PN reduction could be obtained by increasing Γ (e.g. MPE reduced to 25°), but this inevitably resulted in a lower output SNR. The degradation in output SNR at larger Γ is a consequence of the pump fluctuations. This seems to suggest a trade-off between optimizing either phase or amplitude regeneration when pump fluctuations are taken into account.

5. Discussion

The results above indicate the capability of the PSA to simultaneously regenerate amplitude and phase. The additional capability of removing timing jitter could be added in a straightforward manner by using a method of optical clock recovery to retime the pulsed pump. In experiments the case of pump and signal having similar pulse shape and duration has been studied, corresponding to regeneration of signals in dispersion-compensated systems. However other researches have pointed out the usefulness of PSA's as dispersion compensating elements [24], signifying that pulse shapes as well as amplitudes and phases can be restored. When a pulsed pump is used to regenerate broadened signal pulses energy outside the pump envelope is not amplified, which improves the extinction ratio of the signal. The output signal pulse shape closely matches that of the pump, which can be designed appropriately for further transmission.

The seemingly harmless level of pump noise depicted in Fig. 6(a) was enough, when combined with such a highly degraded signal as shown in Fig. 6(b), to present limitations to regeneration performance. When the PSA acts as a regenerator the effects of pump fluctuations are magnified, since for example the phase noise of the pump and signal may combine. Examining the histogram in Fig. 6(c) closely reveals that although the vast majority of the 400 bits considered emerge with nearly the same amplitude, the distribution reaches a lower limit near 0.5 on the normalized scale. These low amplitudes result directly from the combination of small pump phase noise with maximum signal phase errors and small input amplitudes. When the signal degradation is not as severe as in the present experiments the impact of pump fluctuations on regeneration performance is strongly reduced. The impact of pump impairments can also be reduced through variations of the PSA design. Using intensity modulators to generate the DPSK pump eliminates phase errors and incurs minimal amplitude. A more sophisticated phase-locking technique would virtually eliminate the effects of pump PN even at the levels present in this experiment. Practical PSA-based regenerators require an independent pump source phase locked to the incoming DPSK signal; however methods for providing frequency and phase locking for carrier-suppressed modulation formats such as DPSK are already available [25]. Such techniques can easily surpass the phase-locking accuracy achieved here. The need for pump phase modulation can be eliminated through use of emerging ultra-high nonlinearity fibers such as Bismuth-Oxide based fibers, which will not suffer significant SBS and have nonlinear coefficients greater than 1000 $W^{-1}km^{-1}$. It has already been shown that a PPLN-based Mach-Zehnder interferometer, possibly with an integrated frequency doubling stage for generating the 2ω pump, is a good candidate for achieving phase regeneration and could achieve simultaneous amplitude regeneration if the pumping power were high enough [26].

Finally, some comments are in order regarding the noise imposed on the signal for these experiments. In DPSK systems at moderate transmission distances, ASE noise is dominant, which leads to a Gaussian distribution of amplitudes and uniform distribution of the phase.

Visualized on the constellation diagram, the degraded signal exhibits equal noise variances on each of its orthogonal quadratures. At longer distances amplitude noise is converted to nonlinear phase noise, which strongly increases the phase noise variance without affecting the distribution of amplitudes. In that case the strongest and weakest signal bits will have phases farthest from the average phase. In our experiments deterministic noise was generated by applying sinusoidal modulation of the amplitude and phase. Examination of Fig. 6(b) confirms the most interesting combinations of amplitude and phase are well-represented. The results conclusively showed that even the worst-case combinations of amplitude and phase could be effectively regenerated, which also signifies the effectiveness of the regenerator in dealing with nonlinear phase noise. While experiments with ASE-type noise applied would be interesting for practical considerations, we note that previous simulation results indicate such noise can be removed effectively [17, 19]. In fact, the regeneration performance should improve in that case since the PN variance is smaller for a similar SNR.

6. Conclusions

We have demonstrated, for the first time, simultaneous DPSK phase-and-amplitude regeneration using a NOLM-based phase-sensitive amplifier. Such regenerators can be used as inline amplifiers for DPSK transmission systems as they not only reduce the accumulation of phase noise directly but also indirectly because of reduced amplitude fluctuations. The operation of the PSA is highly robust with respect to input signal to noise ratio and phase noise, and improvement in both phase and amplitude statistics is the largest reported improvement in DPSK signal quality to date. Furthermore, measurements of the signal constellation diagram by linear optical sampling give the first directly measured results for DPSK phase regeneration and allow detailed investigations into the operation of the PSA. Maximum phase errors were reduced from 82° to less than 41° with a simultaneous SNR improvement of nearly 6 dB.